

Cardiomyocytes Contractile Activity on Poly(vinyl-alcohol)/Bioglass Electrospun Scaffolds

Subjects: Materials Science, Biomaterials

Contributor: Karla Gómez-Lizárraga, Ricardo Vera Graziano

Tissue scaffolds are generally used as three-dimensional structural supports destined to mimic the morphological structure and function in regeneration processes. Still, beyond this, they are expected to perform the physiological functions for which each tissue or organ is intended. In the case of cardiac tissue, it brings oxygen through the blood to each part of the body through the contraction of the cardiac muscle cells (cardiomyocytes). This contraction is neurologically stimulated through a voltage and calcium-dependent process denominated excitation-contraction coupling, which is mediated by several factors. In this sense, the composition of the scaffold becomes relevant.

Keywords: Contractile activity ; electrospun scaffolds ; cardiomyocytes ; PVA ; bioglass type 58S

1. Introduction

Myocardial infarctions and other diseases of the cardiopulmonary system are considered high-risk diseases due to the high mortality rate in the world population ^[1]. The field of tissue engineering promotes the manufacturing of three-dimensional tissue scaffolds that promote biocompatibility, adhesion, and cell culture through natural, synthetic, or a blend of both polymeric materials and bioactive agents. Electrospinning makes it feasible to approach fibrillar structure, high porosity, and a high surface area-to-volume ratio to mimic the cardiac extracellular matrix of tissues.

To mimic the mechanical and surface properties of the cardiac tissue to be regenerated, hybrid organic/inorganic scaffolds were developed using natural biopolymers ^{[2][3][4][5][6][7][8] [9][10][11]}. PVA membranes have also been designed for the treatment of vascular emboli due to their biocompatibility and low protein adsorption ^[12].

On the other hand, bioglasses have been used since the second half of the last century as bioactive components in tissue engineering to stimulate angiogenesis. The most successful was Bioglass 45S5 ^[13]. Bulk bioglasses are rigid, but in the form of microparticles mixed with ad hoc organic polymers, they enhance the mechanical properties of the polymer. Most bioglasses contain calcium ions (Ca²⁺), among others. Ca²⁺ ions in cardiac tissue affect functions that enable blood circulation in the body. Muscle contractions are a function of intracellular Ca²⁺ levels in cardiomyocytes, and a decrease in these ions reduces myocardial conductivity and the development of cardiovascular disease ^{[14][15]}.

Electrospun scaffolds made of conventional polymers lack suitable mechanical and electrical properties. Therefore, the synchronous beating rate of cardiac cells cultured on these conventional materials has not been achieved ^{[16][17]}.

2. Methodology

The experimental methodology involves four stages:

- Synthesis of bioglass nanoparticles using the sol-gel technique.

The synthesis of bioglass 58S was realized according to the report by Bui, X.V. et al. ^[18], with slight modifications (**Figure 1**).

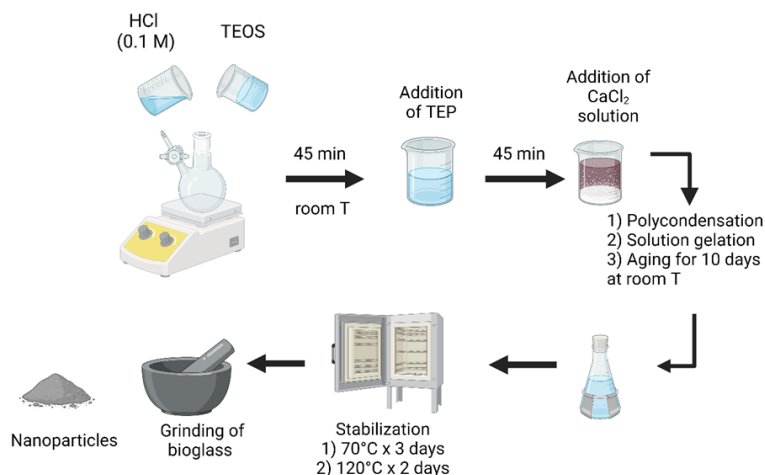


Figure 1. Bioglass 58 S sol-gel synthesis.

A solution of hydrochloric acid (HCl) 0.1 M was mixed with tetraethyl orthosilicate (TEOS) for 45 min at room temperature; then, a triethyl phosphate (TEP) was poured into it with stirring. After 45 min, a solution of calcium chloride dihydrate ($\text{CaCl}_2 \cdot 2\text{H}_2\text{O}$) was added and maintained by stirring for 45 min until the reaction was complete. After ten days, it proceeded to the polycondensation phase, solution gelation, and aging. Finally, the thermal stabilization stages were carried out for 5 days at two temperatures and grounded in an agate mortar to obtain nanometric particles.

- Manufacturing of the hybrid PVA/bioglass scaffold by electrospinning.

As is shown in **Figure 2**, the PVA/bioglass (Bg) solution at different ratios of Bg was electrospun into scaffolds [19].

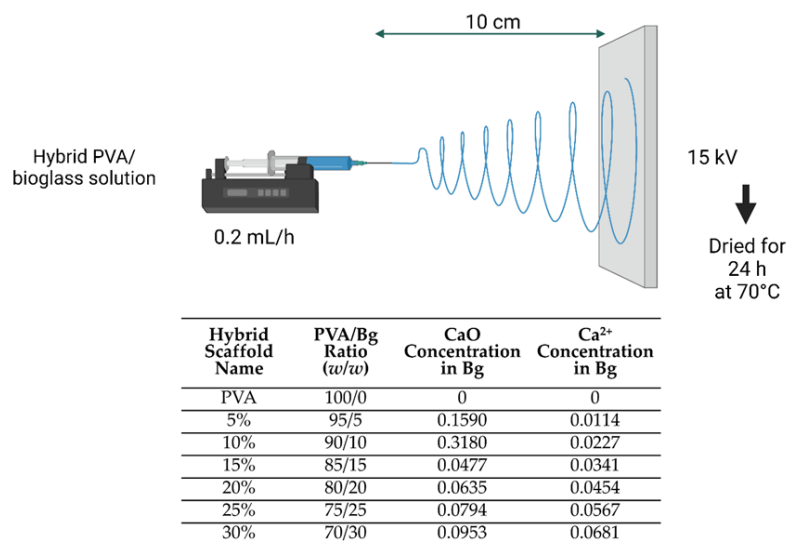


Figure 2. Electrospinning of PVA and hybrid scaffolds.

The conditions for electrospinning PVA and hybrid scaffolds were spinneret needle size and thickness of 0.7×30 mm 22 G, spinneret-collector distance of 10 cm, volumetric flow rate of 0.2 mL/h, an applied voltage of 15 kV. After fabrication, the electrospun scaffolds were dried in a vacuum oven for 24 h at 70°C.

- Chemical crosslinking of scaffolds.

For chemical crosslinking, a mixture of HCl and a solution of glutaraldehyde (25%v/v) with toluene was stirred vigorously, and after the chemical reaction, the phases were separated [20]. As is shown in **Figure 3**, the electrospun hybrid scaffolds were immersed in the upper part of the funnel; this is a glutaraldehyde and toluene mixture. After chemical crosslinking, the electrospun hybrid scaffolds were dried in a vacuum oven for 24 h at 70°C and stored until characterization.

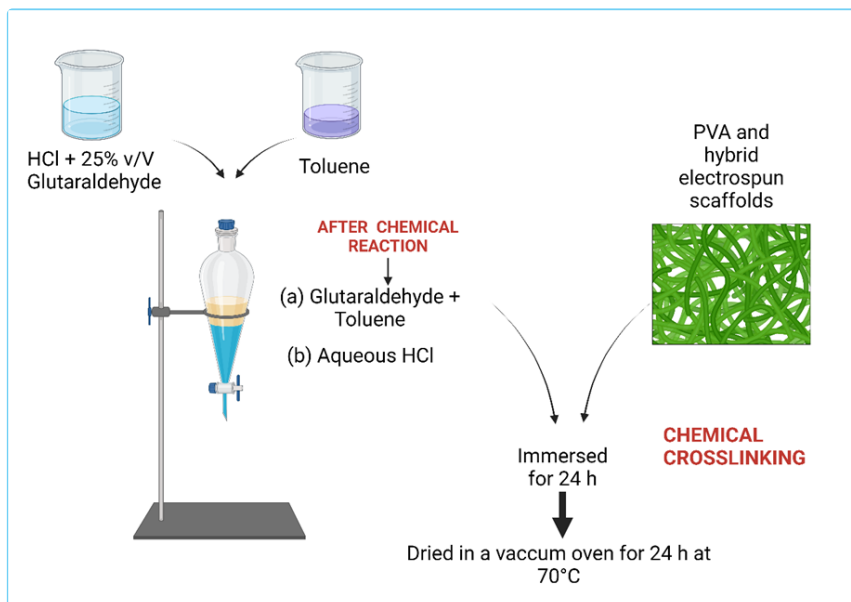


Figure 3. Crosslinked PVA hybrid Scaffolds.

- Physicochemical and biological characterization of electrospun hybrid scaffolds.

Before the biological evaluation, the physicochemical characterization of the scaffolds was carried out before and after crosslinking (Figure 4).

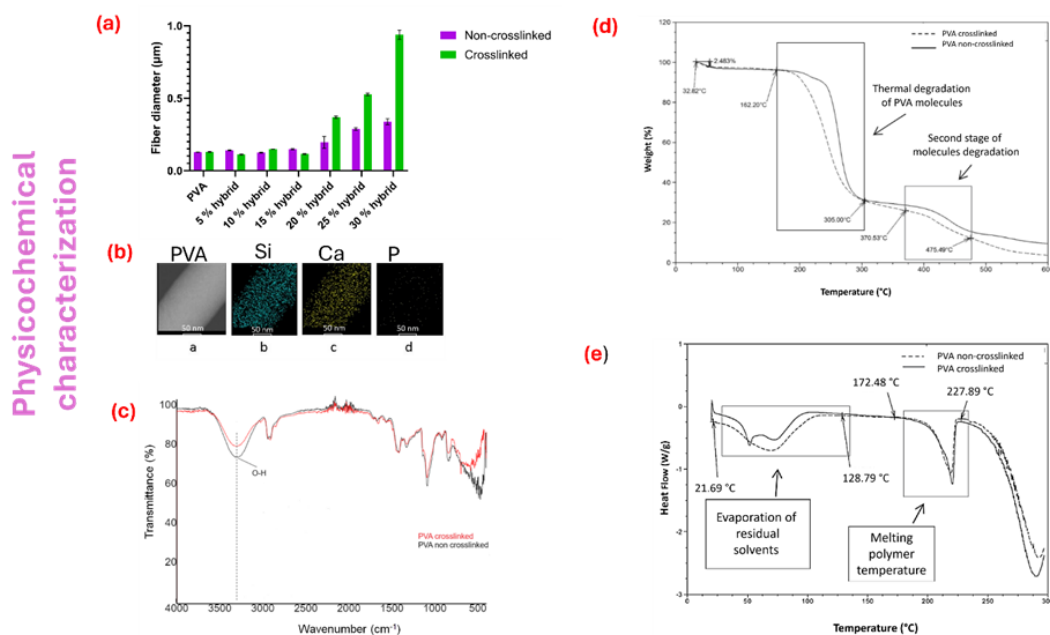


Figure 4. Physicochemical characterization. (a) average fiber diameter of PVA hybrid scaffolds; (b) Elemental bioglass composition in PVA electrospun fiber; (c) FTIR spectra before and after crosslinked; (d) TGA thermogram and (e) DSC thermogram.

Among the properties that were evaluated are the morphology of the electrospun fibers using scanning electron microscopy (SEM), as well as the determination of the average diameter size of the fibers. On the other hand, using transmission electron microscopy (TEM), the presence and incorporation of bioglass nanoparticles in the electrospun fibers were analyzed by energy dispersive X-ray spectrometry (EDX) to determine the presence of the elements Si, Ca, and P. By a Fourier transform infrared spectroscopy with attenuated total reflectance (FTIR-ATR) spectrometer were analyzed the chemical composition of the electrospun scaffolds and determined the bands corresponding to chemical crosslinking [21], [22], [23]. The thermal behavior of the scaffolds was evaluated with thermogravimetric analysis (TGA) [24] and differential scanning calorimetry (DSC). Where the thermal stability associated with weight loss and the thermal transitions corresponding to i) glass transition (T_g) [25][26][27][28][29][30][31], ii) evaporation temperature (T_{Ev}), mainly due to residual water or organic solvents present in the cross-linking reaction, and iii) melting temperature (T_m).

3. Fluorescence Studies Showing the Contractile Activity of the Cells on the Scaffolds

Isolated primary embryonic chick cardiomyocytes were cultured according to previously established procedures [32][33][34][35][36] on the PVA/Bg scaffolds to analyze their effects on cardiomyocyte survival, adhesion, and contractile activity patterns. Dishes containing cardiomyocyte-seeded scaffolds with media were incubated in a 5% CO₂ atmosphere for up to 48 h at 37 °C. Spontaneous cell contractility was observed at 36 °C as the first sign of cell survival by ocular inspection on a microscope stage using a Leica MZ75 fluorescence stereomicroscope; this activity may persist for several days. Calcium Green-1 fluorophore was used to detect intracellular calcium fluctuations (ΔCa^{2+}).

Video images were analyzed by extracting fluorescence amplitude fluctuations in different regions of interest (ROI). Cell images showing contractile activity were outlined with red dots (Figure 5). Fluorescence intensity was plotted as a function of time.

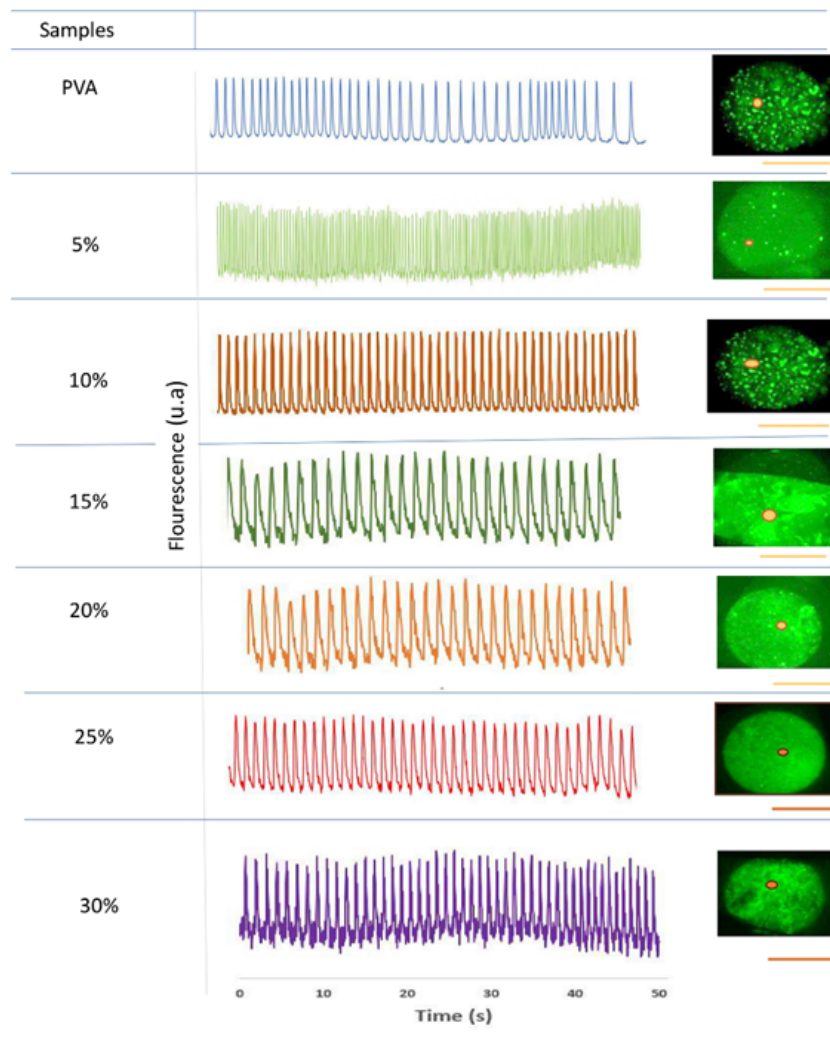


Figure 5. Contractile activity patterns revealed by fluorescence peaks attributable to intracellular ΔCa^{2+} .

Figure 5 shows the contraction pulse sequence in embryonic cardiomyocytes applied to crosslinked scaffolds at different Bg concentrations. At Bg concentrations below 20 %, cells developed in independent niches and did not exhibit homogeneous contraction pulses. At Bg concentrations up to 20 %, the cells formed a uniform cell layer in the ROIs and showed a homogeneous sequence of contraction pulsations. Overall, it was observed that the electrical activity patterns in cardiomyocytes seeded on the electrospun scaffolds strongly depend on the Bg concentration, especially on the availability of Ca^{2+} ions.

4. The Role of Calcium Ions in Cardiomyocytes Contractile Activity

In the literature, it has been reported that the concentration of calcium ions is relevant in the extension-contraction coupling process, which allows for the determination of the patterns of contractile activity in cardiomyocyte-type cells. It has been found that the dissolution of calcium ions is dependent on the PVA concentration [37], the pH [38], and the particle size of the bioglass [39]. Based on these tests, a qualitative model is proposed to explain the dissolution of Ca^{2+} ions in

water as a function of time (Figure 6), assuming that all nanofibers decrease their radius uniformly with time. The diagram below represents the dissolution of Ca^{2+} ions from Bg, which increases continuously from zero to a maximum value (t_0 - t_1). After that, the dissolution of Ca^{2+} ions decreases while the radius (r) of the fibers continues to increase by swelling to a maximum (t_2). After t_2 , both Ca^{2+} and the fiber radius decrease at different rates until t_3 , where both rates become similar, followed by the complete dissolution of the fibers.

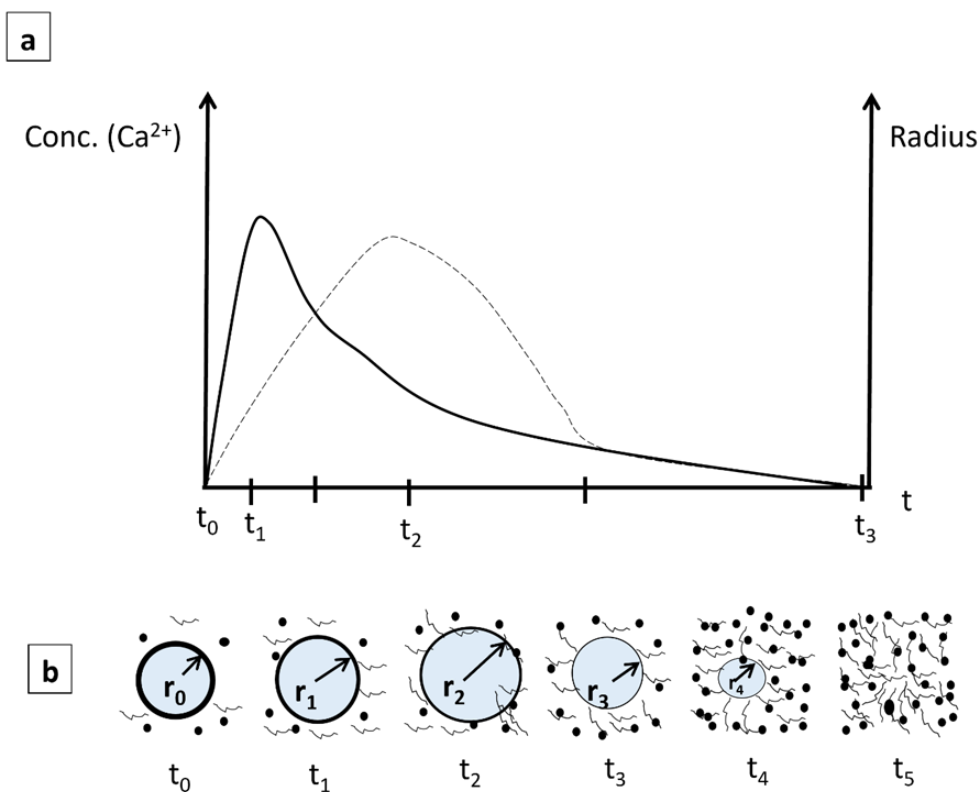


Figure 6. (a) Diagrams of dissolution of Ca^{2+} ions and fiber radius versus time: dissolution of Ca^{2+} , solid line, and fiber radius (r), dotted line. (b) Schematic of the change in fiber radius at different times.

On the other side, the mechanism by which ionic migration of Ca^{2+} to the interior of the cytoplasmic membrane occurs is shown schematically in Figure 7. After contact with the scaffold, cardiomyocytes adhere to the hydrophilic nanofiber surface; this adhesion is further enhanced by releasing Si^{2+} , Ca^{2+} , and PO_4^{3-} ions. When these ions dissolve in the culture medium, they interact with the cardiomyocytes across their cytoplasmic membrane. They alter the electrical potential between intracellular and extracellular space by flowing through selective L-type Ca^{2+} channels [40][41].

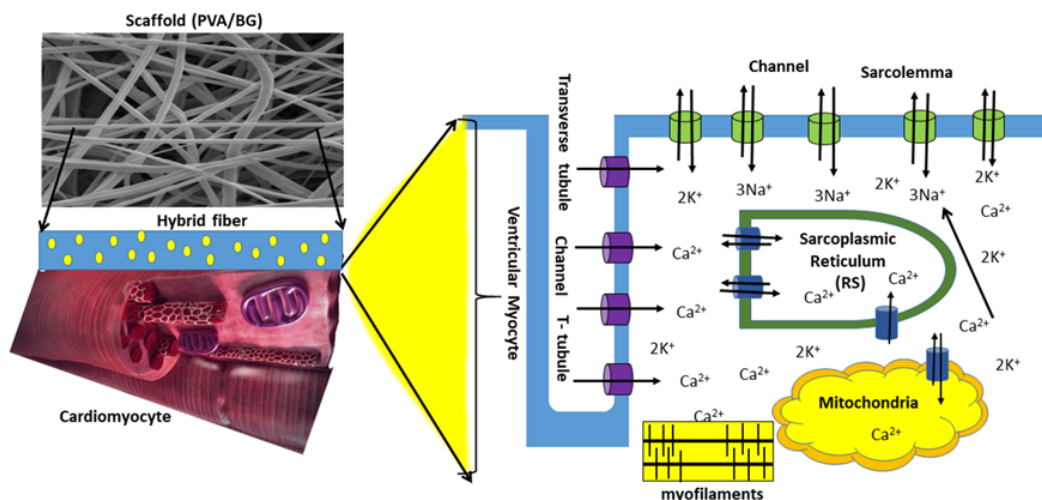


Figure 7. Schematization of cardiomyocytes across the PVA/Bg scaffold surface.

5. Concluding Remarks

Finally, this summary describes the main findings and results of the contractile activity of cardiomyocytes cultured on the crosslinked PVA hybrid scaffolds due to the dissolution of Ca²⁺ ions. Some of the most relevant points are highlighted below:

-The sol-gel technique used here to synthesize Bg made it possible to obtain nanoparticles with 5–20 nm diameters, facilitating their uniform incorporation into fibers with diameters ranging from 130 nm to 340 nm.

-Chemical crosslinking of PVA and increasing the Bg concentration allowed the hybrid nanocomposite scaffolds to stabilize thermally.

-Intracellular calcium fluctuations appear to be associated with increased Bg concentration of releasing Ca²⁺ and Si²⁺ ions.

-Electrospun fiber scaffolds with up to 20 % Bg concentration allowed the formation of a strongly connected cell layer covering the entire scaffold surface, suggesting high cell adhesion and favoring a homogeneous, synchronous, and periodic contractile activity.

References

1. Saeid Kargozar; Sepideh Hamzehlou; Francesco Baino; Potential of Bioactive Glasses for Cardiac and Pulmonary Tissue Engineering. *Mater.* **2017**, *10*, 1429.
2. Marc N. Hirt; Arne Hansen; Thomas Eschenhagen; Mayourian J; Ceholski D; Gonzalez D; Cashman T; Sahoo S; Hajjar R; Costa K; Borovjagin A; Ogle B; Berry J; Zhang J; Taylor D; Chandler A; Gobin A; Sampaio L; Weinberger F; Mannhardt I; Eschenhagen T; Qin X; Riegler J; Tiburcy M; Zhao X; Chour T; Ndoye B; Nguyen M; Adams J; Ameen M; Denney T; Yang P; Nguyen P; Zimmermann W; Wu J; Pijnappels D; Schlij M; Atsma D; de Vries A; Wolfram-Hubertus Zimmermann; Michael Didié; Gerald H. Wasmeier; Uwe Nixdorff; Andreas Hess; Ivan Melnychenko; Oliver Boy; Winfried L. Neuhuber; Michael Weyand; Alexa Whorowski; Joseph C. Wu; Florian Weinberger; Ingra Mannhardt; Helen M. Nugent; Elazer R. Edelman; Cardiac Tissue Engineering. *Circ. Res.* **2014**, *114*, 354-367.
3. Maria Kitsara; Onnik Agbulut; Dimitrios Kontziampasis; Yong Chen; Philippe Menasché; Fibers for hearts: A critical review on electrospinning for cardiac tissue engineering. *Acta Biomater.* **2017**, *48*, 20-40.
4. Zhi Cui; Baofeng Yang; Ren-Ke Li; Application of Biomaterials in Cardiac Repair and Regeneration. *Eng.* **2016**, *2*, 141-148.
5. Emil Ruvinov; Smadar Cohen; Alginate biomaterial for the treatment of myocardial infarction: Progress, translational strategies, and clinical outlook. *Adv. Drug Deliv. Rev.* **2016**, *96*, 54-76.
6. Zhiqiang Liu; Haibin Wang; Yan Wang; Qiuxia Lin; Anning Yao; Feng Cao; Dexue Li; Jin Zhou; Cuimi Duan; Zhiyan Du; Yanmeng Wang; Changyong Wang; The influence of chitosan hydrogel on stem cell engraftment, survival and homing in the ischemic myocardial microenvironment. *Biomater.* **2012**, *33*, 3093-3106.
7. Karen L. Christman; Hubert H. Fok; Richard E. Sievers; Qizhi Fang; Randall J. Lee; Fibrin Glue Alone and Skeletal Myoblasts in a Fibrin Scaffold Preserve Cardiac Function after Myocardial Infarction. *Tissue Eng.* **2004**, *10*, 403-409.
8. Rajesh Lakshmanan; Uma Maheswari Krishnan; Swaminathan Sethuraman; Polymeric Scaffold Aided Stem Cell Therapeutics for Cardiac Muscle Repair and Regeneration. *Macromol. Biosci.* **2013**, *13*, 1119-1134.
9. Valeria Chiono; Pamela Mozetic; Monica Boffito; Susanna Sartori; Emilia Gioffredi; Antonella Silvestri; Alberto Rainer; Sara Maria Giannitelli; Marcella Trombetta; Daria Nurzynska; Franca Di Meglio; Clotilde Castaldo; Rita Miraglia; Stefania Montagnani; Gianluca Ciardelli; Polyurethane-based scaffolds for myocardial tissue engineering. *Interface Focus*. **2014**, *4*, 20130045.
10. Plackett, D.; Vázquez, A. Green Composites: Polymer Composites and the Environment; Baillie, C.; Jayasinghe, R., Eds.; Woodhead Publishing: Sawston, UK, 2004; pp. 123–153 .
11. Rusha Chaudhuri; Madhumitha Ramachandran; Pearl Moharil; Megha Harumalani; Amit K. Jaiswal; Biomaterials and cells for cardiac tissue engineering: Current choices. *Mater. Sci. Eng. C*. **2017**, *79*, 950-957.
12. Elbadawy A. Kamoun; Xin Chen; Mohamed S. Mohy Eldin; El-Refaie S. Kenawy; Crosslinked poly(vinyl alcohol) hydrogels for wound dressing applications: A review of remarkably blended polymers. *Arab. J. Chem.* **2015**, *8*, 1-14.
13. Alsharabasy Am; A Mini-Review on the Bioactive Glass-Based Composites in Soft Tissue Repair. *Bioceram. Dev. Appl.* **2018**, *8*, 1-4.

14. Yaping Ding; Wei Li; Teresa Müller; Dirk W. Schubert; Aldo R. Boccaccini; Qingqing Yao; Judith A. Roether; Electrospun Polyhydroxybutyrate/Poly(ϵ -caprolactone)/58S Sol–Gel Bioactive Glass Hybrid Scaffolds with Highly Improved Osteogenic Potential for Bone Tissue Engineering. *ACS Appl. Mater. Interfaces*. **2016**, *8*, 17098-17108.
15. Donald M. Bers; Calcium Fluxes Involved in Control of Cardiac Myocyte Contraction. *Circ. Res.* **2000**, *87*, 275-281.
16. Marwa Tallawi; Ranjana Rai; Aldo. R. Boccaccini; Katerina E. Aifantis; Effect of Substrate Mechanics on Cardiomyocyte Maturation and Growth. *Tissue Eng. Part B: Rev.* **2015**, *21*, 157-165.
17. María Luisa Durán-Pastén; Hortensia G. González Gómez. Recurrence plots to analyze the dynamical changes during moderate hypothermia in a cell model of reentry; AIP Publishing: Melville, NY, United States, 2019; pp. 050005.
18. Xuan Vuong Bui; Tan Hiep Dang; Bioactive glass 58S prepared using an innovation sol-gel process. *Process. Appl. Ceram.* **2019**, *13*, 98-103.
19. Yanbao Li; Song Yao; High stability under extreme condition of the poly(vinyl alcohol) nanofibers crosslinked by glutaraldehyde in organic medium. *Polym. Degrad. Stab.* **2017**, *137*, 229-237.
20. María Luisa Durán-Pastén; Daniela Cortes; Alan E. Valencia-Amaya; Santiago King; Gertrudis Hortensia González-Gómez; Mathieu Hautefeuille; Cell Culture Platforms with Controllable Stiffness for Chick Embryonic Cardiomyocytes. *Biomimetics*. **2019**, *4*, 33.
21. Herman S. Mansur; Carolina M. Sadahira; Adriana N. Souza; Alexandra A.P. Mansur; FTIR spectroscopy characterization of poly (vinyl alcohol) hydrogel with different hydrolysis degree and chemically crosslinked with glutaraldehyde. *Mater. Sci. Eng. C*. **2008**, *28*, 539-548.
22. Christina Tang; Carl D. Saquing; Jonathon R. Harding; Saad A. Khan; In Situ Cross-Linking of Electrospun Poly(vinyl alcohol) Nanofibers. *Macromol.* **2009**, *43*, 630-637.
23. Katia C. S. Figueiredo; Tito L. M. Alves; Cristiano P. Borges; Poly(vinyl alcohol) films crosslinked by glutaraldehyde under mild conditions. *J. Appl. Polym. Sci.* **2008**, *111*, 3074-3080.
24. Mohammad Taghi Taghizadeh; Narges Sabouri; Thermal Degradation Behavior of Polyvinyl Alcohol/Starch/Carboxymethyl Cellulose/ Clay Nanocomposites. *Univers. J. Chem.* **2013**, *1*, 21-29.
25. Osiris W. Guirguis; Manal T. H. Moselhey; Thermal and structural studies of poly (vinyl alcohol) and hydroxypropyl cellulose blends. *Nat. Sci.* **2012**, *04*, 57-67.
26. J. Rault; R. Gref; Z.H. Ping; Q.T. Nguyen; J. Néel; Glass transition temperature regulation effect in a poly(vinyl alcohol) —water system. *Polym.* **1995**, *36*, 1655-1661.
27. Mohammad Taghi Taghizadeh; Nazanin Yeganeh; Mostafa Rezaei; The investigation of thermal decomposition pathway and products of poly(vinyl alcohol) by TG-FTIR. *J. Appl. Polym. Sci.* **2015**, *132*, 42117.
28. A. Stavropoulou; K. G. Papadokostaki; M. Sanopoulou; Thermal properties of poly(vinyl alcohol)—solute blends studied by TMDSC. *J. Appl. Polym. Sci.* **2004**, *93*, 1151-1156.
29. Kai Huang; Shu Cai; Guohua Xu; Mengguo Ren; Xuexin Wang; Ruiyue Zhang; Shuxin Niu; Huan Zhao; Sol–gel derived mesoporous 58S bioactive glass coatings on AZ31 magnesium alloy and in vitro degradation behavior. *Surf. Coatings Technol.* **2014**, *240*, 137-144.
30. Juliano Zanela; Ana Paula Bilck; Maira Casagrande; Maria Victória Eiras Grossmann; Fabio Yamashita; Polyvinyl alcohol (PVA) molecular weight and extrusion temperature in starch/PVA biodegradable sheets. *null*. **2018**, *28*, 256-265.
31. Zheng Peng; Ling Xue Kong; A thermal degradation mechanism of polyvinyl alcohol/silica nanocomposites. *Polym. Degrad. Stab.* **2007**, *92*, 1061-1071.
32. L. Oropeza-Ramos; A. Macias; S. Juarez; A. Falcon; A. Torres; M. Hautefeuille; H. Gonzalez. Low cost micro-platform for culturing and stimulation of cardiomyocyte tissue; Institute of Electrical and Electronics Engineers (IEEE): Piscataway, NJ, United States, 2011; pp. 912-915.
33. Hortensia González; Yoshihiko Nagai; G. Bub; Leon Glass; Alvin Shrier; Reentrant waves in a ring of embryonic chick ventricular cells imaged with a Ca²⁺ sensitive dye. *Biosyst.* **2003**, *71*, 71-80.
34. Hortensia González; Yoshihiko Nagai; Gil Bub; Leon Glass; Alvin Shrier; Resetting and Annihilating Reentrant Waves in a Ring of Cardiac Tissue: Theory and Experiment. *Prog. Theor. Phys. Suppl.* **2000**, *139*, 83-89.
35. Gil Bub; Leon Glass; Nelson G. Publicover; Alvin Shrier; Bursting calcium rotors in cultured cardiac myocyte monolayers. *Proc. Natl. Acad. Sci.* **1998**, *95*, 10283-10287.
36. E. Miranda-Buendia; G.H. González-Gómez; M.A. Falcón-Neri; M.L. Durán-Pastén; C. Jiménez-Martínez; R. Vera-Graziano; A. Ospina-Orejarena; F. Rivera-Torres; G. Prado-Villegas; A. Maciel-Cerda; Activity patterns of

cardiomyocytes in electrospun scaffolds of poly (ϵ -caprolactone), collagen, and epicatechin. *Mater. Today Commun.* **2022**, *31*, 103405.

37. Adeyinka Aina; Andrew Morris; Manish Gupta; Nashiru Billa; Neesha Madhvani; Ritika Sharma; Stephen Doughty; Vivek Shah; Yamina Boukari; Dissolution behavior of poly vinyl alcohol in water and its effect on the physical morphologies of PLGA scaffolds. *Pharm. Biosci. J.* **2014**, *2*, 01-06.
38. Muriel Józó; Nóra Simon; Lan Yi; János Móczó; Béla Pukánszky; Improved Release of a Drug with Poor Water Solubility by Using Electrospun Water-Soluble Polymers as Carriers. *Pharm.* **2021**, *14*, 34.
39. Marta Giulia Cerruti; David Greenspan; Kevin Powers; An analytical model for the dissolution of different particle size samples of Bioglass® in TRIS-buffered solution. *Biomater.* **2005**, *26*, 4903-4911.
40. Guy Vassort; Karel Talavera; Julio L. Alvarez; Role of T-type Ca²⁺ channels in the heart. *Cell Calcium*. **2006**, *40*, 205-220.
41. Andreas Lieb; Nadine Ortner; Jörg Striessnig; C-Terminal Modulatory Domain Controls Coupling of Voltage-Sensing to Pore Opening in Cav1.3 L-type Ca²⁺ Channels. *Biophys. J.* **2014**, *106*, 1467-1475.

Retrieved from <https://encyclopedia.pub/entry/history/show/125796>